ISSN 0023-1584, Kinetics and Catalysis, 2010, Vol. 51, No. 2, pp. 312–317. © Pleiades Publishing, Ltd., 2010.
Original Russian Text © Ch.N. Barnakov, A.P. Kozlov, A.I. Romanenko, N.T. Vasenin, V.F. Anufrienko, Z.R. Ismagilov, 2010, published in Kinetika i Kataliz, 2010, Vol. 51, No. 2, pp. 330–335.

Synthesis and Properties of a Microporous Carbon Material As a Catalyst Support for Fuel Cells

Ch. N. Barnakov[a], A. P. Kozlov[a], A. I. Romanenko[b], N. T. Vasenin[c], V. F. Anufrienko[c], and Z. R. Ismagilov[c]

[a] *Institute of Carbon and Carbon Chemistry, Siberian Branch, Russian Academy of Sciences, Kemerovo, 650099 Russia*
[b] *Institute of Inorganic Chemistry, Siberian Branch, Russian Academy of Sciences, Novosibirsk, 630090 Russia*
[c] *Boreskov Institute of Catalysis, Siberian Branch, Russian Academy of Sciences, Novosibirsk, 630090 Russia*
e-mail: han@kemnet.ru

Received April 16, 2009

Abstract—It is stated that one-dimensional conductivity in amorphous microporous carbon material (AMCM) samples is associated with the considerable imperfection of graphene fragments in the carbon material rather than the presence of unshared electrons. It is likely that the graphene fragments are formed upon the carbonization of a carbon precursor accompanied by the partial or complete removal of precursor heteroatoms. It is hypothesized that the presence of localized unpaired electrons, which give EPR spectra, is due to the formation of local defects in carbene fragments. Thus, the effects of the value of conductivity and the concentration of unpaired electrons on the power output of a fuel cell cannot be distinguished based on the experimental data with the use of an AMCM as a catalyst support. The interaction of localized paramagnetic centers with electron gas can be interpreted in terms of the C–S relaxation model.

DOI: 10.1134/S0023158410020217

INTRODUCTION

Previously [1], we found that the power output of a fuel cell in which a new amorphous microporous carbon material (AMCM) was used as a catalyst support was higher than that with the use of a Vulcan XC-72R standard support or structurally different nanofibrous carbon materials at the same platinum content (0.02–0.09 mg/cm^2) of the cathode and a platinum particle size of 2–4 nm. The main difference of the AMCM from the Vulcan XC-72R support and nanofibrous carbon materials is that it exhibits one-dimensional hopping conduction and a high concentration (10^{19}–10^{20} spin/g) of unpaired electrons. In this case, Barnakov et al. [2] found that the Curie law was not obeyed for the EPR spectra of the above samples: as the measurement temperature was decreased, the integrated intensity noticeably decreased rather than increased. Barnakov et al. [2] hypothesized that processes occurring at the cathode of a fuel cell are sensitive to these properties of AMCMs. The question now arises of to what extent the above properties are characteristic of AMCM samples and in what cases they can appear in carbon cokes.

The EPR spectra of the free radicals of carbon materials (singlet lines without HFS with $\Delta H = 1$–10 G and $g = g_e$) were first recorded long ago [3]. As a rule, such EPR spectra are observed for coals, cokes, and pyrolysis products of organic compounds (sugar). The integrated intensity of these spectra usually obeys the Curie law, and the line width depends only slightly on the measurement temperature. After the detection of the EPR spectra of coals and cokes sensitive to adsorbed oxygen [4–6], it became clear that the appearance of electron gas upon pyrolysis has a considerable effect on the spectra. This effect is due to the exchange interaction of localized centers (C) with electron gas (S) (C–S relaxation). The physical principles of the C–S relaxation for systems with a degenerate three-dimensional electron gas have been adequately developed [7, 8]. The detection of a sharp broadening of the EPR spectra of Fe^{3+} ions in a matrix of V_2O_4 [9] provided a support for the C–S relaxation. The V_2O_4 oxide is well known as a system with the Mott dielectric–metal transition as the temperature is increased above 280 K. At this temperature, the EPR spectra of Fe^{3+} ions with localized electrons are dramatically broadened.

Unfortunately, the temperature dependence of the spin–lattice relaxation time τ_{SL} remained unknown in the case of coals and cokes. The effect of the C–S relaxation on the EPR spectra of carbon structures has been considered in detail [7]. In the description of this relaxation mechanism, the temperature dependence of the relaxation time τ_{SL}, where L is the lattice, is of paramount importance. There was good reason to believe that this relaxation time depends on the dimension of electron gas in the resulting carbon structure and the number of electrons in the electron gas responsible for its degeneracy. To solve all of these problems, it was necessary to measure the temperature

Synthesis conditions, specific surface areas, and conductivities (at 300 K) of AMCM samples

No.	Precursor	Carbonization temperature, °C	Carbonization time, min	Specific surface area, m^2/g	Conductivity, σ (300 K), $(\Omega/cm)^{-1}$
1*	Phenol and 1,2,3-benzotriazole	900	23	1800	0.06
2*	Phenol and 1,2,3-benzotriazole	700	15	2200	1.06
3*	Phenol and 1,2,3-benzotriazole	900	15	2900	4.95
4	*o*-Nitroaniline and 1,2,3-benzotriazole	700	20	470	0.0002
5	Sample no. 4	900	10	490	0.78
6	8-Hydroxyquinoline and 1,2,3-benzotriazole	700	80	3400	0.33
7	Sample no. 6	900	10	3300	3.32
8	PVC	700	25	2300	0.005
9	Pine nut shells	700	15	2075	1.62

* The synthesis and properties of these samples were described elsewhere [2, 10].

dependence of the conductivity of carbon structures depending on the synthesis methods. It has long been noted [3] that the EPR spectra were not observed if the pyrolysis temperature of coals or organic compounds (sugar) was increased above 700°C; this was likely due to the interaction of localized centers (C), which give EPR spectra, with the formed electron gas (S). The specific characteristics of the electron gas remained unclear.

The aim of this work was to study the electric conductivity and EPR spectra of AMCM samples, which can be used as catalyst supports for fuel cell cathodes.

EXPERIMENTAL

It is well known that the properties of a carbon material depend on its precursor and pyrolysis conditions. For this purpose, we synthesized carbon material samples from various precursors. The common feature of all of the synthesized samples was the occurrence of electric conductivity, although the temperature dependences were different. The AMCM samples were synthesized in accordance with patented procedures [10, 11]. The following organic compounds with various degrees of aromaticity and containing various functional groups were used as sample precursors: phenol, 1,2,3-benzotriazole, *o*-nitroaniline, and 8-hydroxyquinoline, as well as the synthetic and natural polymer materials—poly(vinyl chloride) (PVC) and Siberian pine nut shells. Preliminary communications concerning the studies of test samples have been published elsewhere [2, 12–14].

The table summarizes the main conditions of the synthesis of AMCM samples.

Sample no. 1 was prepared by the carbonization of a mixture of phenol and 1,2,3-benzotriazole in a molar ratio of 2 : 1. Sodium hydroxide was used as an alkali at an organic matter to alkali ratio of 1.76. The carbonization was performed in a closed crucible (in a carbonization gas atmosphere). After cooling, the sample was washed with water to a neutral reaction and dried in air at 110–120°C to constant weight.

Sample no. 2 was obtained under the same conditions as sample no. 1 except for the mixture carbonization temperature and time.

Sample no. 3 was prepared from the same components as sample no. 1, but the organic matter to alkali ratio was 5.0.

A mixture of *o*-nitroaniline and 1,2,3-benzotriazole in a molar ratio of 2 : 1 was used as a precursor for sample no. 4. Sodium hydroxide was used as an alkali in an organic matter to alkali ratio of 1.25. The subsequent treatment was the same as with sample no. 1.

Sample no. 5 was obtained by the repeated carbonization of sample no. 4 in a closed crucible. After the carbonization, the crucible was cooled in air to room temperature.

A mixture of 8-hydroxyquinoline and 1,2,3-benzotriazole in a molar ratio of 1 : 1 was used as a precursor for sample no. 6. Sodium hydroxide was used as an alkali in an organic matter to alkali ratio of 2.5. The sample was carbonized in a closed crucible, and the subsequent treatment was performed as specified for sample no. 1.

Sample no. 7 was prepared after the repeated carbonization of sample no. 6 in a closed crucible. After the carbonization, the crucible with the sample was cooled to room temperature, as with sample no. 5.

To synthesize sample no. 8, commercial S-7059M PVC was used; it was mixed with an aqueous equimolar mixture of potassium and sodium hydroxides in a weight ratio of 1 : 5. The mixture was evaporated and carbonized; the subsequent treatment was performed as specified for sample no. 1.

To synthesize sample no. 8, Siberian pine nut shells were used; they were mixed with a concentrated aqueous solution of potassium hydroxide in a weight ratio of 1 : 2. The mixture was evaporated and carbonized. Then, the sample was treated as specified for sample no. 1.

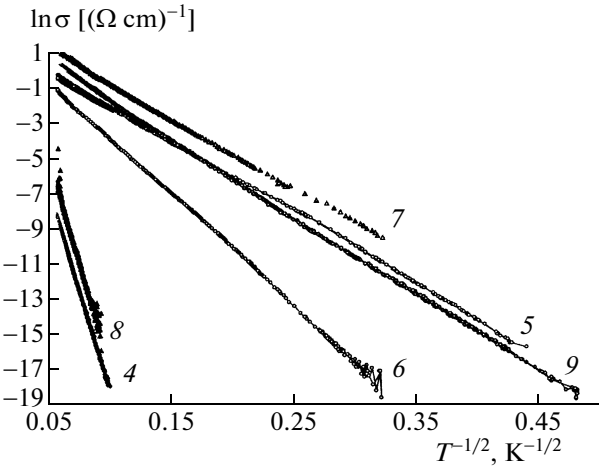

Fig. 1. The temperature dependence of the logarithm of the electric conductivity of AMCM sample nos. 4–9.

The texture characteristics of the resulting AMCM samples were determined on an ASAP-2400 instrument (Micromeritics) using the adsorption of nitrogen at 77 K after the pretreatment of the samples at 300°C away from atmospheric air at a residual pressure of <0.001 Torr until the termination of gas evolution. Then, nitrogen adsorption isotherms were measured at relative pressures from 0.005 to 0.995 and processed in accordance with a standard procedure to calculate the overall surface area (S_{sp}) using the BET method. The EPR spectra were measured on a Bruker ER-200 D spectrometer at 77 and 293 K ($\lambda = 3$ cm) after evacuation at 200°C. The temperature dependence of the conductivity of samples was measured using a four-contact method over the temperature range of 4.2–300 K. The samples as powders were pressed in ampoules. Silver wire 0.1 mm in diameter was used as a contact wire, and powder in the ampoule was pressed to contact the sample with the wire. Raman spectra were recorded on a DILOR OMARS 89 spectrometer with an LN/CCD-1100 PB multichannel detector (Princeton Instruments) and a holographic zero filter. The green line of an ILA-120 argon laser (Carl Zeiss) with a wavelength of 514.5 nm was used as the excitation line. The beam power was 200 mW. The spectra were recorded using an unfocused laser beam lest the power should not burn.

RESULTS AND DISCUSSION

The possibility of conductivity electron localization in a restricted structure region can result in the hopping conduction of current carriers between these localization regions. As the temperature is increased, ordinary hopping conduction between the nearest localization centers is changed by variable-range hopping conduction (VRHC) and described by the generalized Mott law [8]

$$\sigma_{VRHC}(T) = \sigma_0 \exp(-B/T)^{1/(d+1)},$$

where d is the dimension of current carrier migration, $B = [16\alpha^3/k_B N(E_F)]$, α is the reciprocal of the length at which the atomic wave function amplitude decays, $N(E_F)$ is the density of states on the Fermi surface, and σ_0 is a constant.

Figure 1 shows the temperature dependence of the electric conductivity of AMCM sample nos. 4–9. The temperature dependences of the electric conductivities of these samples are noticeably different. However, over the entire test temperature range, the conductivity is described by the relationship corresponding to the Mott law for a one-dimensional case ($d = 1$)

$$\sigma(T) = \sigma_0 \exp(-T_0/T)^{1/2},$$

where $T_0 = [16\alpha/k_B N(E_F) L_\parallel L_\perp^2]$ and $1/\alpha \sim 8$–10 Å [15].

Note that one-dimensional conductivity accompanied by the temperature dependence analogous to that shown in Fig. 1 was observed previously in carbon structures with carbyne chains [16–20]. As can be seen in Fig. 1, the one-dimensional conductivity depends on the nature of the initial carbonization products. Among the above samples, the AMCM sample prepared from Siberian pine nut shells exhibited one-dimensional conductivity over the broadest temperature range (4.2–300 K). The narrowest range (150–300 K) of the temperature dependence of conductivity was observed in the AMCM sample prepared from PVC at a carbonization temperature of 700°C. An increase in the carbonization temperature resulted in an increase in the initial one-dimensional conductivity (σ_0) of the carbon material. In this case, the time of carbonization at 900°C should be no longer than 10–15 min. If the time of carbonization is longer than 20 min, the one-dimensional conductivity of the carbon material changes to the three-dimensional one, which is described by the following relation corresponding to the Mott law for a three-dimensional case ($d = 3$):

$$\sigma(T) = \sigma_0 \exp(-T_0/T)^{1/4} \text{ [2, 14]}.$$

Previously [2, 12–14], we hypothesized that one-dimensional conductivity in our samples was associated with the presence of carbyne. To test this hypothesis, we measured the Raman spectra of sample nos. 7 and 9 with the use of a green laser. Unfortunately, we failed to detect the spectrum of carbyne. It is likely that the one-dimensional conductivity is due to the considerable imperfection of graphene particles in the carbon material, which is formed upon the removal of nitrogen in the course of the carbonization of a carbon precursor. In the cases when PVC or pine nut shells serve as a precursor, it is likely that the formation of defect graphene fragments results from the removal of chlorine or oxygen atoms, respectively.

The table summarizes data on changes in the conductivity (σ) of samples at 300 K. As noted previously,

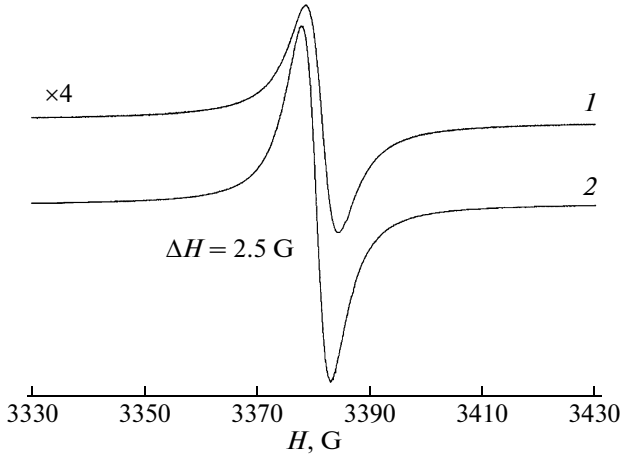

Fig. 2. EPR spectra of evacuated sample no. 4 at (*1*) 293 K room temperature and (*2*) 77 K liquid nitrogen temperature.

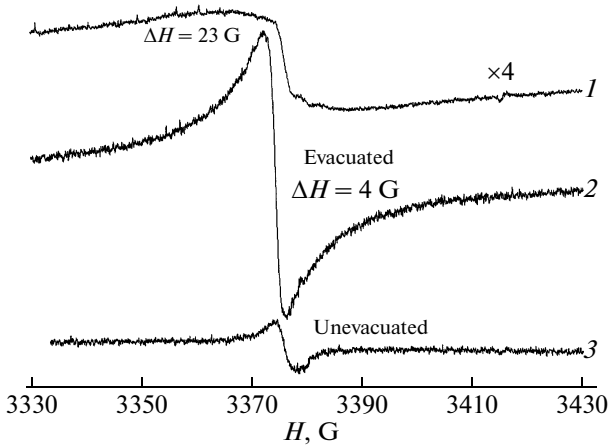

Fig. 3. EPR spectra of evacuated sample no. 6 at (*1*) room temperature, (*2*) liquid nitrogen temperature, and (*3*) unevacuated sample no. 6 at liquid nitrogen temperature.

sample no. 4 exhibited an EPR spectrum. As the initial one-dimensional conductivity (σ) increased, the EPR spectrum broadened, and sample no. 5 did not exhibit an EPR spectrum. Such a behavior was also observed in sample nos. 6 and 7, as well as nos. 2 and 3.

Previously [14], it was noted that sample no. 1 did not exhibit EPR spectra. In evacuated sample nos. 2 and 3, symmetrical EPR spectra with $g = g_e$ were observed. The integrated intensity of all of the EPR spectra was as high as 10^{19} spin/g. It was found that the spectra of these samples, which were shown in [14], as well as the spectra of sample nos. 4 and 6 (Figs. 2, 3) after evacuation, obeyed the Curie law typical of isolated or weakly interacting paramagnetic centers: as the measurement temperature was decreased, the integrated intensity not only did not increase, but it noticeably decreased. It was noted previously [12, 13] that the EPR spectra were broadened upon the repeated carbonization of these samples at 900°C for 10–15 min. It was found that the Curie law was also not obeyed in sample nos. 8 and 9 but in the opposite direction, as compared with sample nos. 2–4 and 6. For example, after the vacuum pumping of sample no. 8 (Fig. 4), a good EPR spectrum of coke with $\Delta H = 5.5$ G was observed, and this spectrum disappeared after opening the ampoule. Its temperature dependence did not obey the Curie law: as the temperature was decreased to 77 K, the intensity increased by a factor of ~15 rather than 4 according to the Curie law; that is, the Curie law violation was opposite to that in the above case of sample nos. 2–4 and 6. This was likely due to different natures of the starting materials.

The found special features of the temperature dependence of the EPR spectra can be understood using the C–S relaxation model [8, 16]. This model (see the scheme) takes into account the effect of the exchange interaction of electron gas (S) with localized centers (C) on the width of the EPR signal of the localized centers. From the narrow neck model ($\tau_{SC} < \tau_{SL}$) for the C–S relaxation, it follows [8, 16] that the width of the EPR spectrum of the localized center (C) is determined by the following expression:

$$\Delta H \approx \frac{\rho(E_F)kT}{N_C}\frac{1}{\tau_{SL}},$$

where $\rho(E_F)$ is the density of electronic states on the Fermi surface; N_C is the concentration of the localized centers (C); τ_{SL} is the spin–lattice relaxation time of electron gas (S); and k is Boltzmann's constant.

Note that the value of τ_{SL} for a three-dimensional electron gas strongly depends on temperature [8, 15, 16] ($1/\tau_{SL} \sim T^n$, where $n = 4$–7 for various models). Thus, in the case of a one-dimensional electron gas for sample no. 8, the EPR spectra of a portion of localized centers, which are strongly broadened at 300 K, dramatically narrow as the temperature is decreased; this is equivalent to a greater increase in the EPR signal intensity with decreasing temperature than that follows from the Curie law ($I \approx C/T$, where C is a constant).

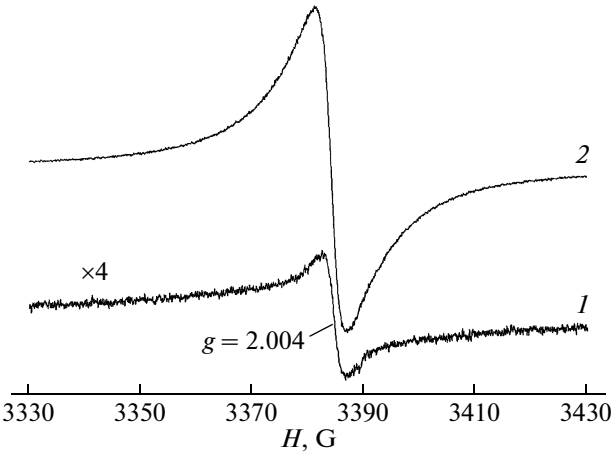

Fig. 4. EPR spectra of evacuated sample no. 8 at (*1*) room temperature and (*2*) liquid nitrogen temperature.

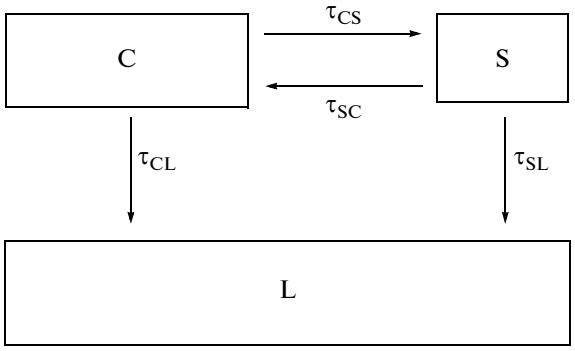

Schematic diagram of C–S relaxation: (C) are localized electrons, (S) is electron gas, L is the crystal lattice, and τ_{CS}, τ_{SC}, τ_{SL} are the relaxation times.

It is likely that, as the measurement temperature is decreased, the electron localization of electron gas on defects in sample no. 8 weakens the exchange interaction of localized centers (C) and electron gas (S). That is, in this case at a low temperature (77 K), the C–S relaxation model is completely excluded and the "pure" EPR spectrum of localized centers (C) is observed. The inverse relation between the EPR spectrum intensity and temperature, which was found in sample nos. 2–4 and 6, can also be understood. Physically, it is clear than the temperature dependence of the line width ΔH depends on the properties of electron gas. There is good reason to believe that the localization of a portion of electron gas near localized centers (C) occurs as the temperature is decreased; this results in a noticeable broadening of the EPR spectra of centers (C)—the disappearance of spectra as the temperature is decreased.

The found special features of the effect of the properties of electron gas on the EPR spectra of carbon structures should be studied in more detail.

CONCLUSIONS

We found that the one-dimensional conductivity of a carbon material is not necessarily associated with the presence of unshared electrons, but it is caused by the considerable imperfection of graphene fragments in the carbon material. In the case of a nitrogen-containing carbon material, this imperfection results from the partial or complete removal of nitrogen atoms in the course of carbonization. In the cases that PVC or pine nut shells serve as an AMCM precursor, it is likely that the imperfection of graphene fragments results from the removal of chlorine or oxygen atoms, respectively. It is believed that localized unpaired electrons, which give an EPR spectrum, are associated with the formation of local defects in the graphene fragments of AMCMs. The samples exhibit an EPR spectrum when the number of one-dimensional conductivity carriers is small. As the number of carriers increases with the retention of one-dimensional conductivity, the EPR spectrum broadens. The EPR spectrum can also broaden because of a change of the one-dimensional conductivity of the carbon material to the three-dimensional conductivity. Thus, based on the experimental results, we cannot distinguish between the effects of the conductivity and the concentration of unpaired electrons upon the change in the power output of a fuel cell, in which an AMCM is used as a catalyst support. The interaction of localized paramagnetic centers with electron gas can be explained in terms of the C–S relaxation model.

ACKNOWLEDGMENTS

This work was supported by the Presidium of the Siberian Branch of the Russian Academy of Sciences (Complex Integration Project SO RAN 2006 no. 4.5), the Russian Foundation for Basic Research (grant no. 07-03-96042), and the Ministry of Education and Science (grant no. RNP.2.1.1.1604).

We are grateful to N.N. Ovsyuk for recording the Raman spectra.

REFERENCES

1. Ismagilov, Z.R., Kerzhentsev, M.A., Shikina, N.V., Lisitsyn, A.S., Okhlopkova, L.B., Barnakov, Ch.N., Masao Sakashita, Takashi Iijima, and Kenichiro Tadokoro, *Catal. Today*, 2005, vols. 102–103, p. 58.
2. Barnakov, Ch.N., Kozlov, A.P., Seit-Ablaeva, S.K., Romanenko, A.I., Vasenin, N.T., Anufrienko, V.F., Ismagilov, Z.R., and Parmon, V.N., *Ross. Khim. Zh.*, 2006, vol. 50, no. 1, p. 54.
3. Ingram, D.J., *Spectroscopy at Radio and Microwave Frequencies*, London: Butterworths, 1955.
4. Sidorov, A.A and Anufrienko, V.F., *Kinet. Katal.*, 1966, vol. 7, p. 1060.
5. Vasil'ev, L.M. and Anufrienko, V.F., *Kinet. Katal.*, 1971, vol. 12, p. 1310.
6. Shklyaev, A.A., Anufrienko, V.F., and Vasil'eva, L.M., *Dokl. Akad. Nauk SSSR*, 1971, vol. 200, p. 1165.
7. Ravilov, R.G., *Cand. Sci. (Phys.–Math.) Dissertation*, Novosibirsk: Inst. of Catalysis, 1980.
8. Mott, N.F. and Davis, E.A., *Electron Processes in Non-crystalline Materials*, Oxford: Clarendon, 1979, 2nd ed.
9. Ioffe, V.A. and Andronenko, R.R., *Fiz. Tverd. Tela*, 1983, vol. 25, p. 2212.
10. RF Patent 2206394, 2003.
11. RF Patent 2307069, 2007.
12. Barnakov, Ch.N., Romanenko, A.I., Kozlov, A.P., Seit-Ablaeva, S.K., Vasenin, N.T., Anufrienko, V.F., and Ismagilov, Z.R., *"Catalysis: Fundamentals and Application," Proc. III Int. Conf.*, Novosibirsk, Russia, 2007.
13. Barnakov, Ch.N., Romanenko, A.I., Kozlov, A.P., Seit-Ablaeva, S.K., Vasenin, N.T., Anufrienko, V.F., and Ismagilov, Z.R., *Proc. Int. Carbon Conf.*, Seattle, Wash., 2007.

14. Kozlov, A.P., Barnakov, Ch.N., Romanenko, A.I., Anufrienko, V.F., Kerzhentsev, M.A., Ismagilov, Z.R., and Parmon, V.N., *Preprint of the 231st ACS National Meeting*, Atlanta, Ga., 2006, FUEL 0121.

15. Joo, J., Long, S.M., Pouget, J.P., Oh, E.J., MacDiarmid, A.G., and Epstein, A.J., *Phys. Rev. B: Condens. Matter*, 1998, vol. 57, p. 9567.

16. Hirst, I.I. and Schafer, W., *Phys. Rev. B: Condens. Matter*, 1973, vol. 8, p. 64.

17. Gossard, A.C., *J. Appl. Phys.*, 1967, vol. 38, no. 1, p. 12.

18. Demishev, S.V., Pronin, A.A., Glushkov, V.V., Sluchanko, N.E., Samarin, N.A., Kondrin, M.V., Lyapin, A.G., Brazhkin, V.V., Varfolomeeva, T.D., and Popova, S.V., *Pis'ma Zh. Eksp. Teor. Fiz.*, 2003, no. 8, p. 984.

19. Shenderova, O.A., Zhirnov, V.V., and Brenner, D.W., *Crit. Rev. Solid State Mater. Sci.*, 2002, vol. 27, nos. 3–4, p. 227.

20. Sladkov, A.M. *Karbiny – tret'ya allotropnaya forma ugleroda* (Carbynes: The Third Allotropic Form of Carbon), Moscow: Nauka, 2003, p. 151.